Exploring the bronzing effect at the surface of ink layers (Orale)

Mathieu Hébert, Maxime Mallet, Alexis Deboos, Pierre Chavel, Deng-Feng Kuang, Jean-Paul Hugonin, Mondher Besbes, Anthony Cazier

Exploring the bronzing effect at the surface of ink layers

Mathieu Hébert[a,b], Maxime Mallet[b], Alexis Deboos[b], Pierre Chavel[a,c], Deng-Feng Kuang[b,d], Jean-Paul Hugonin[c], Mondher Besbes[c], Anthony Cazier[a,b]

[a]Laboratoire Hubert Curien, Université de Lyon, Université Jean Monnet de Saint Etienne, CNRS, Saint Etienne, France; [b]Institut d'Optique – Graduate School, Saint Etienne, France. [c]Laboratoire Charles Fabry, Institut d'Optique, Université Paris-Sud, CNRS, Palaiseau, France. [d]Key Laboratory of Optical Information Science and Technology (Ministry of Education), Institute of Modern Optics, Nankai University, Tianjin 300071, China

ABSTRACT

We investigate the optical phenomenon responsible for the colored shine that sometimes appears at the surface of ink layers in the specular direction, often called bronzing or gloss differential. It seems to come from the wavelength-dependent refractive index of the ink, which induces a wavelength-dependent reflectance of the ink-air interface. Our experiments on cyan and magenta inkjet inks confirm this theory. Complex refractive indices can be obtained from measurements of the spectral reflectance and transmittance of a transparency film coated with the ink. We propose a correction of the classical Clapper-Yule model in order to include the colored gloss in the prediction of the spectral reflectance of an inked paper. We also explored effects of scattering by the micrometric or nanometric roughness of the ink surface. The micrometric roughness, easy to model with a geometrical optics model, can predict the spreading of the colored gloss over a large cone. Electromagnetic models accounting for the effect of the nanometric roughness of the surface also predict the attenuation of short wavelengths observed under collimated illumination.

Keywords: Bronzing, printing, ink, gloss, complex refractive index.

1. INTRODUCTION

Printing is based on coloring a white reflecting surface through continuous or discontinuous layers of inks. The inks are colored materials, generally non-scattering or weakly scattering, that play a role of spectral filtering. However, it sometimes occurs, especially in inkjet printing, that a colored shine appears in the specular direction whose hue is noticeably different from the color of the ink itself, a well-known phenomenon often called "bronzing" or " gloss differential" by professionals of photo printing, or amateur photographers who print their pictures in inkjet on photo-quality paper. Discussions including recommendations to avoid the effect can be found on the internet in forums specialized in photo printing[1], but a satisfactory physical explanation is elusive, as it also is in the scientific literature on printing sciences and technologies. To our knowledge, the only web page where a sound physical explanation is proposed illustrates the phenomenon in the case of ball pen inks, for which the effect is often pronounced, and analyses the influence of the absorbance of the ink on the reflectance of the air-ink interface[2]. Indeed, the Fresnel formulas directly state that the reflectance of an interface with a difference in the complex relative refractive index is an increasing function of that difference[3]. This applies to the imaginary part of the index, representative of the absorbance of the medium. Our experiments confirm that this phenomenon essentially explains the colored gloss. It also explains why the phenomenon disappears with an overlay, since the air-interface interface is replaced with a air-coating interface.

Beyond our scientific interest for this physical phenomenon, our study was also motivated by its consequences on the accuracy of prediction models in the color reproduction domain. After a description of the phenomenon through color pictures and spectral measurements, where we insist on the importance of the illumination geometry, we recall the Fresnel reflectance formulas for an interface between a clear medium and a medium with complex refractive index. We propose a method to calculate the complex index of the ink from the spectral reflectance and transmittance of a transparency film on which the ink is printed. Then, we review the Clapper-Yule model,[4] a classical reflectance model for inked paper, and develop a correction capable of predicting the colored gloss in the specular direction. More advanced models are evocated but still need to be tested. Finally, the influence of the surface roughness, at microscopic and nanoscopic scales, is analyzed thanks to incoherent and coherent light models.

2. DESCRIPTION OF THE PHENOMENON

The bronzing phenomenon is characterized by a colored sheen that sometimes arises at the surface of ink layers, with a different tint than the tint of the ink itself. The picture displayed in Fig. 1 shows the pinkish sheen displayed by Canon PGI-9C cyan ink printed on the Canon PP-201 Photo Plus glossy paper, whereas the achromatic specular reflection by the paper reveals the yellowish color of the halogen lamp and the inked area illuminated by diffuse light has the expected cyan color. The effect is even more striking in Fig. 2 with the black BIC Cristal ballpoint pen ink for which the gloss is coppered. Bronzing is less striking with the Canon PGI-9M (magenta) and PGI-9Y (yellow) inks, not displayed here but also analyzed in the next sections.

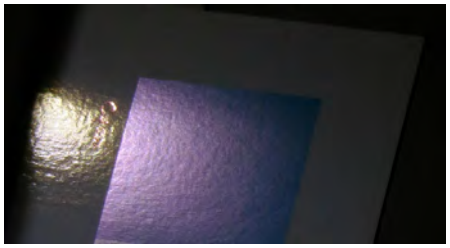

Fig. 1. Picture of a patch of cyan inkjet ink printed on a glossy paper with specular reflection of the white source. On the inked area, the specularly reflected light exhibits a pinkish sheen.

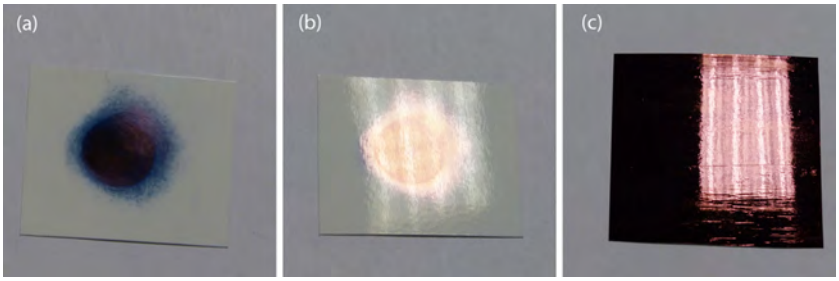

Fig. 2. Two samples of black ballpoint pen ink coated on the a glossy paper: (a-b) a thick layer at the center of the paper, surrounded by a thinner layer, is observed out of (a) and in (b) the specular direction in respect to the lamp; (c) coppered metallic reflection on a thick ink layer covering the paper.

2.1 Spectral measurements

When coating an ink on a transparency film, the bronzing effect occurs only on the inked face, not the other one. This suggests that the concerned optical phenomenon occurs at the ink-air interface, not within the ink layer. This is shown in Fig. 3 in which are compared the spectral reflectance factors measured on the inked face and the non-inked face of a 3M transparency film coated with different inks, namely the Canon PGI-9C cyan inkjet ink shown in Fig. 1, and the blue and black BIC Cristal ballpoint pen inks (the black ink being the one shown in Fig. 2). The reflectance factors were measured in the specular direction under a collimated illumination at 45° from the normal of the sample (45°:45° measuring geometry according to the notations recommended by the CIE[5]), with normalization by the unprinted paper measured in the same geometrical configuration. We added the spectral transmittances of the inked films measured in the normal direction in order to give an idea the spectral absorbance of the inks. They are consistent with their respective intrinsic color, cyan, blue and black.

The reflectance factors of the non-inked face of the film (grey lines in Fig. 3) are almost achromatic since they are composed of 1) the achromatic reflectance of the air-film interface at the front side of the film, and 2) the reflectance of the ink-air interface at the back side attenuated by double transmission through the ink layer. The multiple reflections between the two interfaces form an additional component that is small in comparison to the two main ones. The reflectance factors of the inked face of the film (black lines) are higher and their variations according to the wavelength are more pronounced. This is a characteristic of bronzing.

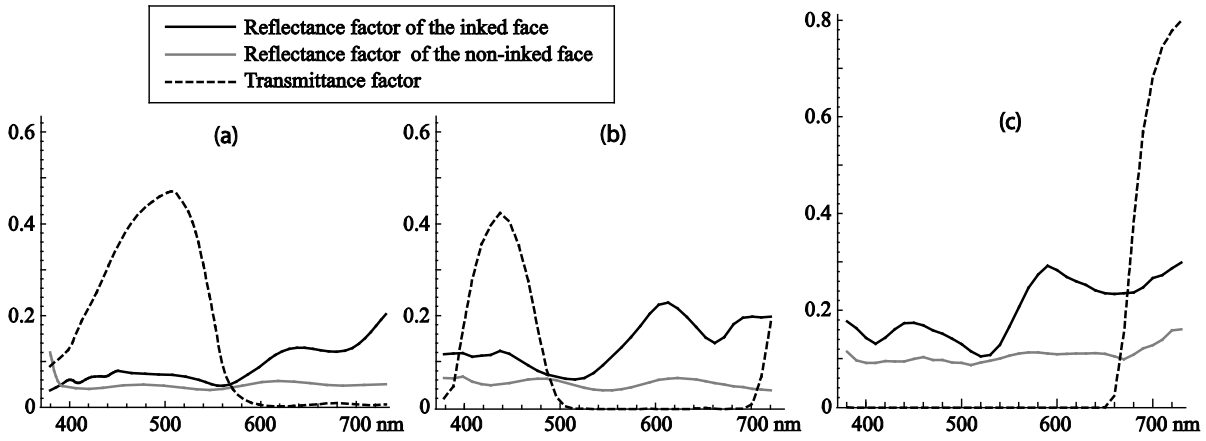

Fig. 3. Spectral reflectance and transmittance factors of a clear film coated with (a) cyan inkjet ink, (b) blue ballpoint pen ink, and (c) black ballpoint pen ink. The spectral reflectance factors are measured in the 45°:45° geometry on the inked and non-inked faces of the film. The spectral transmittances are measured in the normal direction of the film.

In Fig. 4, we compare the spectral reflectance factors of the Canon PP-201 Photo Plus glossy paper coated with the Canon PGI-9C cyan inkjet ink or the black BIC Cristal ballpoint pen ink, either in the specular direction (45°:45° geometry) or an non-specular direction (35°:45° geometry). The non-specular reflectances are consistent with the cyan and black colors of the inks, whereas additional spectral components are observed in the specular direction, beyond 600 nm for the cyan ink, and between 550 nm and 670 nm for the black ink. These spectral domains where the reflectance is increases are consistent with the gloss colors observed in the pictures in Figs. 1 and 2.

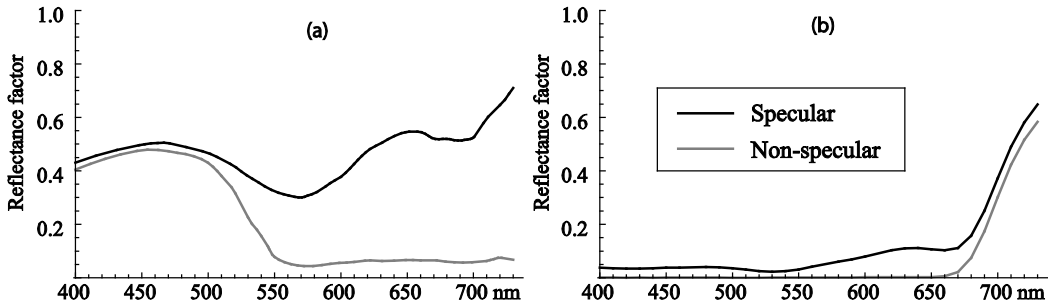

Fig. 4. Spectral reflectance factors of (a) cyan inkjet ink and (b) black ballpoint pen ink on glossy white paper, measured in steps of 10 nm in a 45°:45° geometry (black lines) or a 35°:45° geometry grey lines.

According to these first observations, bronzing clearly seems to be a gloss effect. It is mainly observed in the specular direction, even though the roughness of the ink-air interface may spread it over a wider range of directions.

2.2 Influence of the illumination geometry

One difficulty in the study of bronzing is its dependence on the illumination geometry. In Figure 4.a, we noticed through the example of the glossy paper coated with cyan ink the difference between the reflectance factors measured in and out of the specular direction for a collimated illumination at 45°. The same sample was measured with the X-rite Color i7 spectrophotometer, which illuminates the sample with Lambertian light and captures the reflected radiance at 8° from its normal, either in the specular component included mode (di:8° geometry according to the notation recommended by the CIE[5]) and in the specular component excluded mode (de:8° geometry). The difference between the two spectral reflectance factors, plotted in Fig. 5.a, is much lower than the one observed in Fig. 4.a. Similar measurements performed on the 3M transparency film coated with the same cyan ink are plotted in Fig. 5.b.

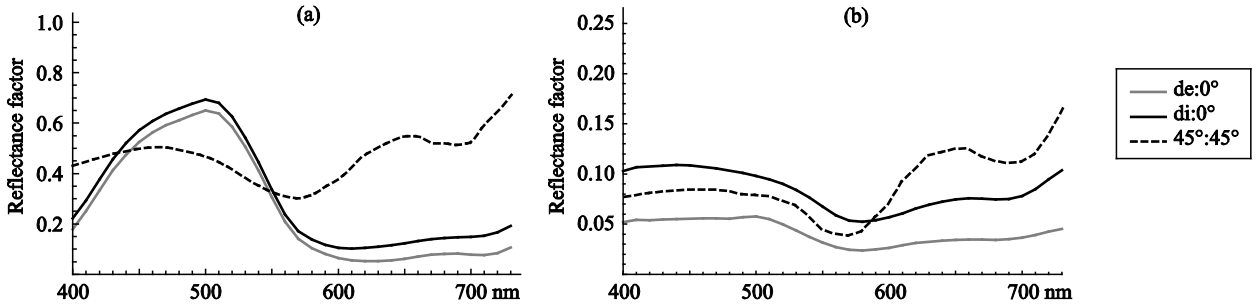

Fig. 5. Spectral reflectance factors of cyan ink coated on (a) glossy white paper and (b) a transparency film, measured in steps of 10 nm in either a de:8° geometry, a di:8° geometry, or a 45°:45° geometry.

The fact that bronzing is stronger under collimated than Lambertian illumination is explained by radiometric considerations related to the illumination and observation geometries[6]. Let us assume, in first approximation, that the inked paper reflects a perfectly diffuse component r_d and its flat surface reflects a perfectly specular component r_s. The incident irradiance is denoted E_i (we omit the dependence on wavelength in order to simplify the notations). The observer captures the reflected radiance in a direction (θ, φ). A perfectly white diffuser reflects the radiance E_i/π in every direction, therefore in the direction of the observer. The inked paper, perfectly diffusing, reflects the radiance $r_d E_i/\pi$ in every direction. In contrast, the flat surface reflects only the radiance coming from the regular direction in respect to the observer, radiance whose contribution to the total irradiance is different according to the illumination geometry.

When the illumination is Lambertian, the incoming radiance in the regular direction is E_i/π, and the radiance perceived by the observer is $r_s E_i/\pi$. Hence, the total reflectance factor of the sample, ratio of the radiance from by the sample to the radiance from by the perfect white diffuser, is

$$R = r_s + r_d \tag{1}$$

When the irradiance E_i comes from an infinitesimal solid angle $d\omega = \sin\theta d\theta d\varphi$, it forms a radiance $E_i/d\omega\cos\theta$. The observer perceives the radiance $r_d E_i/\pi$ diffusely reflected by the inked paper as well as the radiance $r_s E_i/d\omega\cos\theta$ specularly reflected by the surface. The reflectance factor becomes

$$R = \frac{\pi}{d\omega\cos\theta} r_s + r_d \tag{2}$$

For a larger but limited illumination solid angle, $\Delta\omega$, the specular reflectance becomes

$$R = \gamma r_s + r_d \tag{3}$$

with

$$\gamma = \frac{\pi}{\iint_{(\theta,\varphi)\in\Delta\omega} \cos\theta \sin\theta d\theta d\varphi} \tag{4}$$

Notice that Eq. (1) is a special case of Eq. (3) where the illumination solid angle is the hemisphere, therefore $\gamma = 1$. As $\Delta\omega$ becomes thinner, the specular reflectance increases. This is what we observe on the pictures of Figs. 1 and 2 where the specularly reflected light is much brighter that the white paper. However, eventual roughness of the ink-air interface may decrease the glossiness of the surface, therefore the visibility of the colored gloss.

2.3 Diagnostic on the possible origin of the bronzing effect

Bronzing does not occur with every ink. This suggests that the chemical composition of the ink is concerned in the phenomenon. However, a same ink may display the colored sheen on a specular support, but not on a matte or porous one. The spectral reflectances plotted in Fig. 6 show that the difference between the reflectance factors in di:8° and de:8°

modes observed with the Canon PP-201 glossy paper is not observed with the Canon MP101 matte paper coated with the same ink. This confirms the conclusions of Ref. 7 that bronzing does not come from scattering effects taking place within the ink itself (e.g. due to pigments). We should rather consider that the interfaces of the ink layer is concerned. On the matte paper, the air-ink interface is very rough, and ink-paper interface may be transformed into a gradient of ink-paper mixture as the paper penetrates into the paper substrate.

A second observation speaks in favor of interface effects: the sheen disappears when a layer of clear material is coated on top of the ink, even a simple fingerprint. The disappearance of the colored sheen coincides with the replacement of the ink-air interface with the coating-air interface, whose reflectance is almost achromatic.

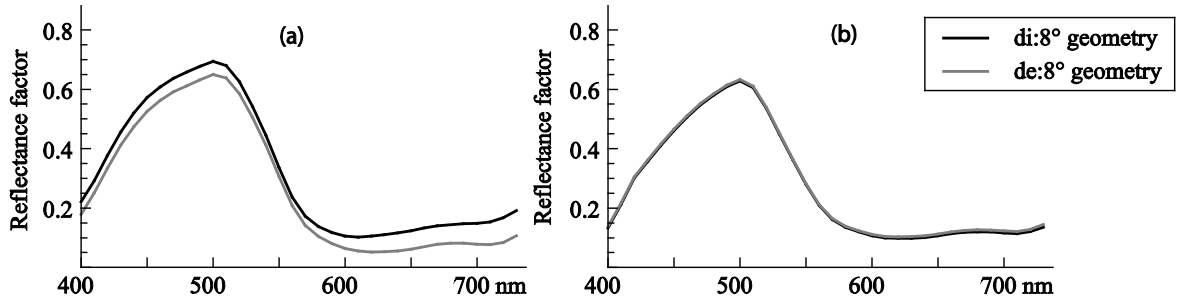

Fig. 6. Spectral reflectance factors of cyan ink solid layer printed on (a) the Canon PP-201 Photo Plus glossy paper and (b) the Canon MP101 matte paper, measured in steps of 10 nm with the X-rite Color i7 spectrophotometer, in Specular Component Included mode (black lines) and Specular Component Excluded mode (grey lines).

A wavelength-dependent refractive index of the inks may explain the wavelength dependent reflectance of the ink-air interface, according to the Fresnel formulae. It is also known that the surface of a strongly absorbing medium, e.g. a metal, increases with the absorbance of the medium. This is well predicted by the Fresnel formulas based on the complex refractive index of the medium, whose imaginary part is related to the absorption coefficient[3]. This first hypothesis will be explored in the Section 3.

Classical reflectance models for inked papers, such as the Williams-Clapper[8] model and the Clapper-Yule model[4], assume that the ink layer and the printing support have the same real optical index. This makes sense when the ink penetrates the support, even partially, because there is no ink-paper interface. However, these models cannot predict bronzing effect in the specular direction, unless the wavelength-dependent complex refractive index of the ink is used to compute the reflectance of the ink-air interface, as we propose in Section 4.2. More advanced models, evocated in Section 4.3, can also be inspired of flux propagation models in multilayers or electromagnetic models for thin films. It is also known that reddish gloss may be observed on a surface with nanometric roughness[9-10] under collimated illumination, due to a coherent scattering by the surface whose magnitude decreases with the wavelength of light. It is therefore more pronounced for blue light than for red light. The consequences of this effect are analyzed in Section 5.2.

3. COMPLEX REFRACTIVE INDEX OF INKS

In the complex refractive index of an absorbing medium, $\hat{n}_i = n_i + i\kappa_i$, the real part n_i represents the classical refractive index and the imaginary part, κ_i, is the extinction index, related to the absorption coefficient at a given wavelength λ according to[3]:

$$\alpha(\lambda) = 4\pi\kappa(\lambda)/\lambda \tag{5}$$

3.1 Fresnel formulas

The Fresnel reflectance at normal incidence of the interface between the absorbing medium and a clear medium with real index n_c is given by:

$$r_{ic} = \frac{(n_i - n_c)^2 + \kappa_i^2}{(n_i + n_c)^2 + \kappa_i^2} \tag{6}$$

Numerical evaluation would show that the reflectance of the interface increases as the extinction coefficient κ_i increases[11]. At oblique incidence of angle θ, the Fresnel reflectance for unpolarized light is given by

$$r_{ic}(\theta) = \frac{1}{2}\left[\frac{\left(\sqrt{a+z}-\cos\theta\right)^2 + a - z}{\left(\sqrt{a+z}+\cos\theta\right)^2 + a - z}\right]\left[1 + \frac{\left(\sqrt{a+z}-\sin\theta\tan\theta\right)^2 + a - z}{\left(\sqrt{a+z}+\sin\theta\tan\theta\right)^2 + a - z}\right] \tag{7}$$

with

$$z = \frac{1}{2}\left[\left(n_i / n_c\right)^2 - \left(\kappa_i / n_c\right)^2 - \sin^2\theta\right] \quad \text{and} \quad a = \sqrt{z^2 + n_i^2\kappa_i^2}\ .$$

Parameters n_i, κ_i, and therefore α and $r_{ic}(\theta)$ are generally functions of wavelength.

3.2 Obtaining the complex refractive index of inks

The usual technique to measure refractive indices is ellipsometry[12]. However, this technique requires very flat surfaces, and the inked surfaces are too rough to use it. Alternatively, we can print the ink on a transparency film and deduce the ink's refractive index from the spectral reflectances and transmittances of the printed film, by using a flux transfer model. The model relies on spectral fluxes, therefore on incoherent light. Interferences are therefore ignored. It takes into account the reflections and transmission of light by the interfaces, and the transmissions through the ink layer and the film layer[13].

We first need to determine the refractive index and the internal transmittance of the film. Since it is very weakly absorbing, we can assume that it has a real refractive index n_f and an internal transmittance $t_f(\lambda)$. Its total transmittance at normal incidence is given by Ref. 14, p. 30:

$$T_f = \frac{16 n_f^2 t_f}{\left(1+n_f\right)^4 - \left(1-n_f\right)^4 t_f^2} \tag{8}$$

and its reflectance at normal incidence is given by

$$R_f = \left(1-n_f\right)^2 \frac{\left(1+n_f\right)^2 - \left(1-6n_f+n_f^2\right)t_f^2}{\left(1+n_f\right)^4 - \left(1-n_f\right)^4 t_f^2} \tag{9}$$

There exists only one solution of equations (8) and (9) for n_f and t_f such that $n_f > 1$ and $0 < t_f < 1$, given by

$$\begin{aligned} n_f &= \frac{1}{T_f A}\left[\left(1 - R_f - T_f\sqrt{A^2+1}\right) - \sqrt{2T_f}\sqrt{A + T_f - \left(1-R_f\right)\sqrt{A^2+1}}\right] \\ t_f &= \sqrt{A^2+1} - A \end{aligned} \tag{10}$$

with

$$A = \frac{\left(1-R_f\right)^2 - T_f^2}{2T_f} \tag{11}$$

By measuring the spectral reflectance and the transmittance of the film at normal incidence, we can directly deduce the refractive index $n_f(\lambda)$ and the internal transmittance $T_f(\lambda)$ in each waveband from equations (10) and (11).

The transparency film coated with an ink of complex refractive index $\hat{n}_i(\lambda) = n_i(\lambda) + i\kappa_i(\lambda)$ has a two-layer structure, containing three interfaces: the ink-air interface, the ink-film interface and the film air interface, whose respective reflectances at normal incidence are

$$r_{0i} = \frac{(n_i - 1)^2 + \kappa_i^2}{(n_i + 1)^2 + \kappa_i^2}; \quad r_{if} = \frac{(n_i - n_f)^2 + \kappa_i^2}{(n_i + n_f)^2 + \kappa_i^2} \quad \text{and} \quad r_{0i} = \frac{(n_f - 1)^2}{(n_f + 1)^2} \tag{12}$$

The internal transmittance of the film is known, and the one of the ink layer depends on the extinction index κ_i according to (5) and Beer's law[14]:

$$t_i = e^{-\alpha h} = e^{-4\pi h \kappa_i / \lambda} \tag{13}$$

where h is the thickness of the ink layer.

Reflectance and transmittance expressions for the coated film can be obtained by describing the multiple reflections and transmissions of light between the two layers and three interfaces. The transfer matrix model detailed in Ref. 13 eases considerably the computations. The obtained expressions for the reflectance R of the coated film on the inked face, the reflectance R' on the non-inked face, and the transmittance T at normal incidence are respectively expressed as:

$$R = r_{0i} + \frac{(1 - r_{0i})^2 \left[r_{if} + r_{f0} (1 - 2 r_{if}) t_f^2 \right] t_i^2}{1 - r_{0i} r_{if} t_i^2 - r_{if} r_{f0} t_f^2 - r_{0i} r_{f0} (1 - 2 r_{if}) t_f^2 t_i^2} \tag{14}$$

$$R' = r_{0f} + \frac{(1 - r_{0f})^2 \left[r_{if} + r_{0i} (1 - 2 r_{if}) t_i^2 \right] t_f^2}{1 - r_{0i} r_{if} t_i^2 - r_{if} r_{f0} t_f^2 - r_{0i} r_{f0} (1 - 2 r_{if}) t_f^2 t_i^2} \tag{15}$$

and

$$T = \frac{(1 - r_{0i})(1 - r_{ik})(1 - r_{f0}) t_f t_i}{1 - r_{0i} r_{if} t_i^2 - r_{if} r_{f0} t_f^2 - r_{0i} r_{f0} (1 - 2 r_{if}) t_f^2 t_i^2} \tag{16}$$

In equations (14), (15) and (16), r_{0i}, r_{ik}, and t_i depend on n_i and κ_i. We can deduce them numerically, for each wavelength, from the measured reflectance R and transmittance T of the coated film.

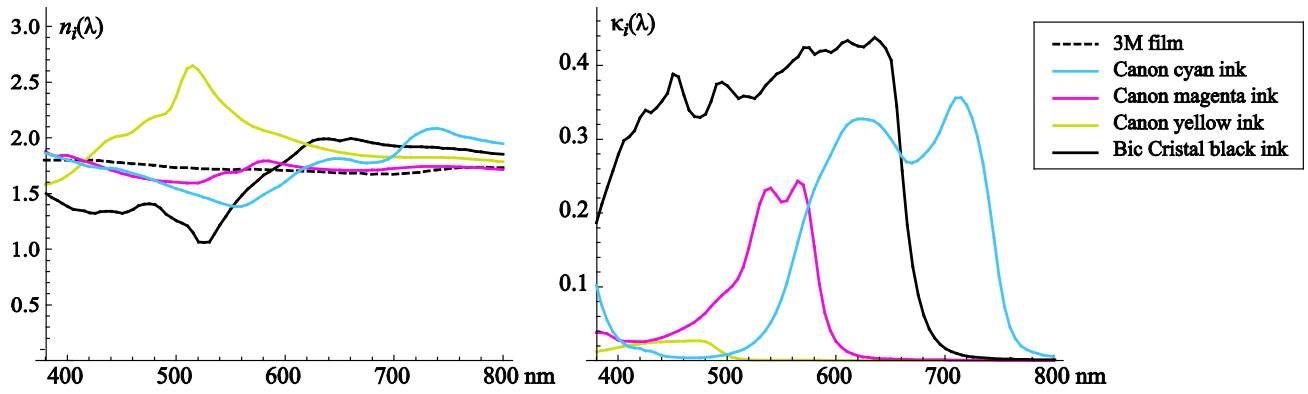

Fig. 7. Real part (left) and imaginary part (right) of the refractive index of inks as a function of wavelength.

Fig. 7 shows the obtained spectral values for the Canon PGI-9C (cyan), PGI-9M (magenta) and PGI-9Y (yellow) inks deposited with the Canon Pixma Pro9500 inkjet printer, as well as for the black BIC Cristal ballpoint pen ink. The ink layer thickness was assumed to be 1 µm for each ink. The spectral measurements where performed in steps of 5 nm by using the Perking-Elmer Lambda 900 spectrophotometer, based on the 0°:diffuse geometry in both reflection and transmission. This geometry is particularly suitable because an integrating sphere collects all the reflected or transmitted flux, therefore includes the scattered flux the interfaces are slightly rough, or the material slight scattering. Omitting the scattered flux in the measurement would provide lower reflectance and transmittance for the inked film, thus yield lower

refractive index n and higher extinction coefficient κ of the media. Moreover, this spectrophotometer has a good signal-to-noise ratio, which is recommended to measure the spectral transmittance of the inked film when the ink is strongly absorbing. Lastly, very coherent light may produce interferences visible in spectra measured in steps of 1 nm (see Section 4.3). Larger bandwidth is therefore preferable in order to prevent oscillated spectra and increase the signal-to-noise ratio.

As expected and confirmed by the highest values of the extinction coefficient $\kappa(\lambda)$, the cyan ink mainly absorbs the red light (600-750 nm), the magenta ink the green light (530-580 nm) and the yellow ink the blue light (below 500 nm). The real refractive indices are clearly wavelength-dependent. We can notice that the real index is also higher in these absorptions bands. However, the peak observed around 510 nm in the $n_i(\lambda)$ curve for the yellow ink is an artifact due to the fluorescence of the ink: the gain in reflectance and transmittance measured on the inked film due to fluorescence are interpreted by the model as a gain in reflectance of the ink-air interface and a loss of transmittance of the ink layer, and therefore has a higher real index of the ink and a lower extinction coefficient. The black Bic Cristal ink is very absorbing, almost opaque, in the visible spectrum. It is not surprising to obtain high extinction index values. We can however notice a slightly lower absorbance in the short wavelength domain explaining the blue tint observed in the picture of Fig. 2.1 where a thin layer of ink is coated on white paper. In contrast, the ink is almost transparent in the near infrared, beyond 700 nm, as indicated by the very low extinction index values in the wavelength domain.

This method to compute the refractive indices is very sensible to the measurement conditions, i.e., geometry and noise. Since the model ignores eventual scattering by the inks and interferences by the ink layers, some errors may be introduced, and a specific study would be necessary to analyze the consequences of these errors on the prediction accuracy of the bronzing effect. The ink thickness must also be estimated. In our experiments, we considered thicknesses of 1 nm. We could also use the oscillations due to interferences[3] observed in the spectra measured in steps of 1 nm (see Section 4.3).

4. REVIEWING THE REFLECTANCE MODELS FOR INKED PAPER

One classical reflectance model for inked papers is the Clapper-Yule model[4]. The original model was developed for halftone colors, but it also applies with solid ink layers by considering a unit surface coverage of the ink. The interest of the model is that it explicitly takes into account the reflections and transmissions of light by the ink-air interface, according to the illumination and observation angles. It assumes that the ink and the support have the same real refractive index; the ink-support interface is therefore optically neutral. The refractive index of the ink and the support is assumed to be a constant over the visible spectrum of light, typically around 1.5. Because of this, the model predicts an achromatic specular reflectance for the ink-air interface. By introducing the complex refractive index, we propose a correction permitting to predict the colored gloss component.

4.1 The Clapper-Yule model

The Clapper-Yule model is a classical reflectance model for halftone prints which enables to predict the spectral reflectance of an inked paper knowing the internal reflectance of the paper and the internal transmittance of the ink layer. The reflections and transmissions of light at the print-air interface are explicitly taken into account. Assuming that the support has an internal reflectance $r_g(\lambda)$ and the ink layer an internal transmittance $t(\lambda)$, the reflectance factor in the normal direction of a paper wholly covered by ink, is expressed according to the Clapper-Yule model as:

$$R(\lambda) = r_s + \frac{T_{in}T_{ex}r_g(\lambda)t^2(\lambda)}{1 - r_i r_g(\lambda)t^2(\lambda)} \tag{17}$$

where the terms T_{in}, T_{ex}, r_s and r_i denote the reflectance and transmittance of the ink-air interface, derived from the Fresnel formulae for unpolarized light according to the lighting and the measuring geometries. The term r_s corresponds to the specular reflectance of the ink-air interface (it is zero if the specular reflection is not captured by the detector). The fraction in Eq. (17) corresponds to the diffuse reflectance of the inked surface.

In the specular direction, r_s is given by:

$$r_s = \left(\frac{1-n_i}{1+n_i} \right)^2 \tag{18}$$

T_{in} is the transmittance for incoming light; for diffuse incident light, the transmittance is obtained by integrating over the hemisphere the Fresnel angular transmittance T_{0i} of the interface at the air side

$$T_{in} = \int_{\theta=0}^{\pi/2} T_{0i}(\theta) \sin 2\theta d\theta \tag{19}$$

T_{ex} is the ratio of radiances before and after crossing the ink-air interface. For an observation in the normal of the print, we have:

$$T_{ex} = \left[1 - \left(\frac{1-n_i}{1+n_i} \right)^2 \right] \frac{1}{n_i^2}$$

where the term $1/n_i^2$ is a consequence of the refraction across the interface on the geometrical extent in which flows the exiting radiance[15]. Finally, r_i is the reflectance of the interface at the ink side for the light diffused by the support[16]:

$$r_i = \int_{\theta=0}^{\pi/2} R_{i0}(\theta) \sin 2\theta d\theta$$

where R_{i0} is the Fresnel angular reflectance of the ink-air interface at the ink side.

By measuring the spectral reflectance factor $R_w(\lambda)$ of the unprinted support, one obtains from (17) with $t = 0$ the internal reflectance of the diffusing support:

$$r_g(\lambda) = \frac{R_w(\lambda) - r_s}{T_{in}T_{ex} + r_i\left(R_w(\lambda) - r_s\right)} \tag{20}$$

Then, by measuring the spectral reflectance factors $R_i(\lambda)$ of the solid colorant patches expressed by Eq. (17), one deduces the intrinsic spectral reflectance of the substrate:

$$t_i(\lambda) = \sqrt{\frac{R_i(\lambda) - r_s}{r_g(\lambda)\left[T_{in}T_{ex} + r_i\left(R_i(\lambda) - r_s\right)\right]}} \tag{21}$$

Through the Fresnel terms T_{in}, T_{ex}, r_s and r_i, the refractive index of the printing materials is present in all equations above. Since the classical Clapper-Yule model assumes that this index is real, around 1.5, it cannot predict a colored gloss. We thus propose a basic correction, before evocating more complex models which should be developed and tested.

4.2 Basic correction of the Clapper-Yule model including the colored gloss effect

In order to account for the colored gloss component in the Clapper-Yule model, we propose a first simple correction, by modifying only the specular reflectance r_s while keeping the diffuse reflectance represented by the fraction in Eq. (17). Instead of calculating r_s with a real index 1.5 according to Eq. (18), we calculate it from Eq. (12) with the complex refractive index obtained in Section 3.2; we also introduce the γ factor defined by Eq. (4) according to the illumination solid angle. The corrected Clapper-Yule equation, in the specular direction, is written:

$$R(\lambda) = \gamma \frac{\left[1 - n_i(\lambda)\right]^2 + \kappa_i^2(\lambda)}{\left[1 + n_i(\lambda)\right]^2 + \kappa_i^2(\lambda)} + \frac{T_{in}T_{ex}r_g(\lambda)t^2(\lambda)}{1 - r_i r_g(\lambda)t^2(\lambda)} \tag{22}$$

where the ink transmittance t, the paper intrinsic transmittance r_g as well as the constants T_{in}, T_{ex}, and r_i have the same meaning as in the classical Clapper-Yule model, and are obtained in the same way.

We tested the classical and corrected Clapper-Yule equations with the PP-201 glossy paper coated with Canon PGI-9 cyan or magenta inks. The considered geometry is the di:8° geometry ($\gamma = 1$). The measured reflectance and the ones

predicted by Eqs. (17) and (22) are plotted in Fig. 8. In order to assess the deviation between the predicted and measured spectra in respect to the human vision, we use the CIELAB ΔE94 color distance metric computed by converting both spectra into CIE-XYZ tristimulus values calculated with a D65 illuminant for the 2° standard observer, and then into CIELAB color coordinates using as white reference the spectral reflectance of the unprinted paper illuminated with the D65 illuminant. For the cyan and magenta inks, the ΔE94 values obtained with the correction were respectively 0.70 and 0.68 unit, whereas those obtained with the classical equation were 1.10 and 1.58 unit. The corrected equation thus improves the prediction accuracy of the Clapper-Yule model. However, we are in the case where the bronzing effect is the weakest because the γ factor is the lowest.

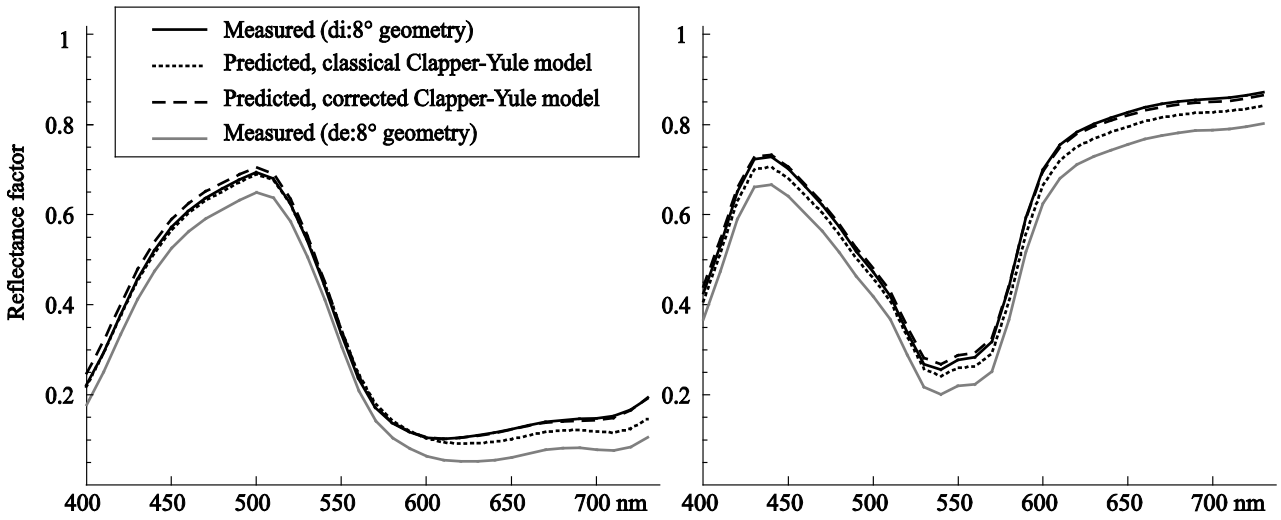

Fig. 8. Spectral reflectance factors of the PP-201 photo paper coated with cyan (left) and magenta (right) inks measured in diffuse:8° geometry with specular component included, and predicted with the classical and corrected Clapper-Yule equations.

Under a collimated illumination, the factor γ is much higher than 1. The inked surface reflects towards the detector a much higher radiance than a perfect diffuser does. This is an issue for accurate measurement of the reflectance factor in respect to the white diffuser. Instead, we defined the reflectance factor in respect to the unprinted glossy paper, whose reflectance is comparable to the reflectance with ink (actually, it is slightly lower, therefore the reflectance factor is higher than one in some spectral domains). The measured and predicted spectra are shown in Fig. 9.

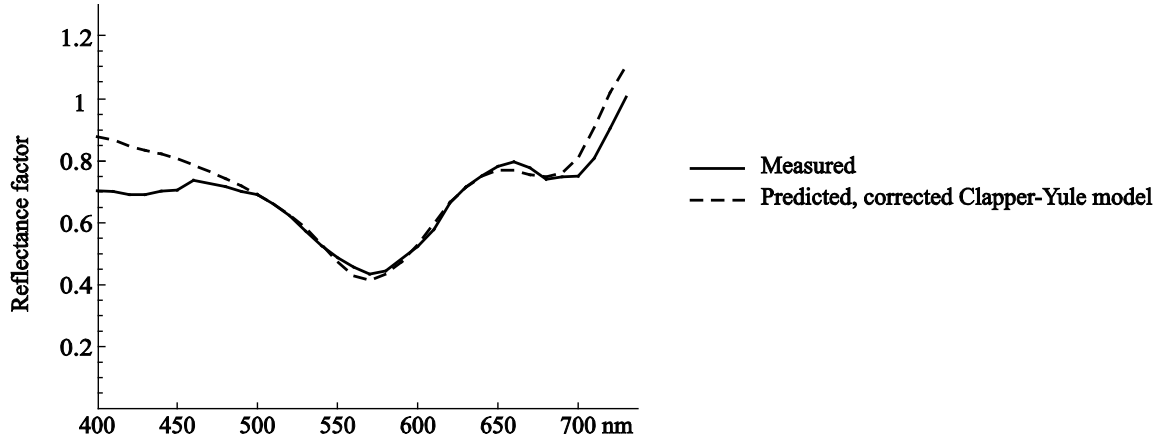

Fig. 9. The spectral reflectance factors of a photo paper coated with cyan ink measured in 45°:45° geometry is compared to the predicted spectral reflectance of the air-ink interface, computed from the complex refractive index of the ink.

For the prediction, since the diffuse reflectance component is much smaller than the specular one, we considered only the specular reflectance of the ink-air interface, computed with the complex refractive index of the cyan ink and with a γ value of 13 fitted in order to obtain the best agreement with the measured reflectance factor. The spectral reflectance factor is rather well matched, despite a strong deviation in the short wavelengths. This deviation is mainly responsible for the high $\Delta E94$ value of 4.35 computed between the measured and predicted spectra. Adding the very small diffuse component makes almost no changing. Possible reasons for this poor prediction in the blue part of the spectrum are 1) some imprecision in the measurement (the power of the used halogen lamp was low in the short wavelengths), 2) some imprecision in the refractive index of the inks, either due to the measurements or the model used to calculate it, which would be emphasized by the high factor γ, or 3) the demonstration that the proposed model is too simplistic to account for all the optical phenomena occurring under collimated light: weshow in Section 5.2 that the nanometric roughness of the air-ink interface can yield comparable attenuation of the gloss in the short wavelength domain.

4.3 Advanced models

The basic correction of the Clapper-Yule model presented in the previous section concerns only the specular reflectance of the air-ink interface. Rigorously, one should also compute the parameters T_{in}, T_{ex}, and r_i from this complex refractive index, which would therefore becomes wavelength-dependent. Moreover, when the ink-support interface physically exists, i.e. the ink has no possibility to penetrate the support, reflections and transmissions of light by it should be explicitly taken into account. The multilayer structure of the inked support is similar to the one considered in Section 3.2 for the inked transparency film, except that the support is diffusing and scatters light in every direction. The extension of the Williams-Clapper model proposed in Ref. 17, extended to complex refractive indices, should apply. Similar extension of the Clapper-Yule model is possible by simply ignoring the orientation of light in the ink layer (the Clapper-Yule model being a non-orientational model in contrast with the Williams-Clapper model that is orientational[18]).

It is also possible that the ink layer is in the order of magnitude of the temporal coherence length of light. In this case, interferences could be observed through oscillations in the reflectance spectrum of the sample, especially under collimated illumination. The spectral reflectance of the cyan ink printed on the photo paper, measured in steps of 1 nm in the 45°:45° geometry, contains these oscillations beyond 600 nm (Fig. 10). In order to predict these interferences, a model based on the thin film theory[19] is necessary: the reflectance and transmittance of the ink layer and its bordering interfaces should be first computed for coherent waves, then integrated over the range of phase angles between waves in order to obtain the reflectance and transmittance for the incoherent fluxes issued from the light source and the diffusing substrate. However, as far as we could see in our experiments, interferences mainly concern red and infrared light and the spectral oscillations have rather small period. A human observer could not see any color difference between the spectra with and without these oscillations. Therefore, a thin film model does not seem mandatory to achieve accurate color prediction with the ink thicknesses usually encountered in ink-based printing.

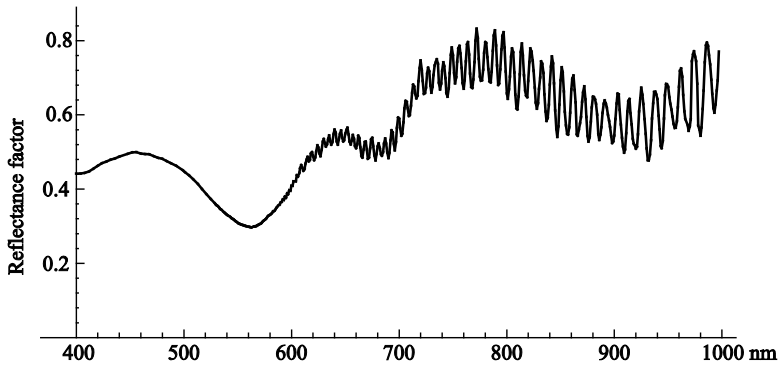

Fig. 10. The spectral reflectance factor of cyan ink printed on glossy paper displays typical oscillations of interferences beyond 600 nm when measured in steps of 1 nm, whereas they were not visible in the spectral reflectances of the same sample, measured in the same geometry but in steps of 10 nm, plotted in Figs. 4.a and 5.a. The amplitude of the oscillations increases with the wavelength, which indicates that the degree of coherence of light also increases with the wavelength.

5. INFLUENCE OF THE SURFACE ROUGHNESS OF THE INKS

The roughness of the air-ink interface may have a significant effect on the perception of bronzing, and on the possible errors it introduces in the classical reflectance prediction models for printed surfaces. Some colored gloss may be captured by the detector even when the measuring geometry should discard the specularly reflected light. This is especially an issue with the diffuse:8° geometry in specular component excluded mode, often used in printing research and applications. The amount of colored gloss that is captured is difficult to estimate, and it may degrade the precision of the spectral reflectances used to calibrate the prediction models. Furthermore, it is known that roughness at the nanometric scale produces reddish specular reflection under collimated illumination, because of electromagnetic scattering. This phonemenon, first considered as the main cause of the bronzing effect, was also investigated.

5.1 Micrometric roughness

Predicting the light scattering by a rough surface whose roughness dimension is larger than the wavelength is rather well known. We can use the Cook-Torrance microfacet model[20], combined with Smith's statistical model[21] in order to account for the shadowing and masking of light at oblique incidence and oblique observation. Both models rely on the same roughness parameter: the standard deviation of the surface's local slope. In a preview study, we proposed an extension of the Clapper-Yule model for rough printing supports, based on these models[11]. As in the classical Clapper-Yule model, we considered a real refractive index for the printing materials. It was shown that the surface roughness as a significant effect on the specular reflectance r_s, but not on the other parameters T_{in}, T_{ex} and r_i. Therefore, in first approximation, we can restrict the use of the scattering model for the computation of the specular reflectance. The Fresnel reflectance of the ink, included into the Cook-Torrance model, is obviously calculated with the complex refractive index of the ink. This provides a second correction of the Clapper-Yule equation

$$R(\lambda) = r_s(\theta_i, \varphi_i; \theta_r, \varphi_r; \lambda) + \frac{T_{in} T_{ex} r_g(\lambda) t^2(\lambda)}{1 - r_i r_g(\lambda) t^2(\lambda)} \tag{23}$$

where $r_s(\theta_i, \varphi_i; \theta_r, \varphi_r; \lambda)$ denotes the angle- and wavelength-dependent reflectance of the rough interface for the considered illumination direction (θ_i, φ_i) and observation direction (θ_r, φ_r). Its spectral power distribution comes from the Fresnel reflectance included in the Cook-Torrance model, which is computed from the spectral refractive index of the ink. This spectral power distribution does not vary significantly according to the angle. In contrast, the nanometric roughness is also responsible for light scattering but with a wavelength-dependent strength (stronger for the blue light).

A light scattering model is probably unnecessary for most applications in color reproduction, but it might be useful to estimate the amount of colored gloss that is captured by the detector, therefore the error introduced in the calibration measurements of reflectance prediction models for printed surfaces.

5.2 Nanometric roughness

Measurements with an atomic force microscope were carried out on a film printed with cyan ink in order to study the roughness of the ink-air interface at the nanometric scale and its impact on the specular reflectance of the inked film. Fig. 11 shows the 2D and 1D roughness profile of the ink surface.

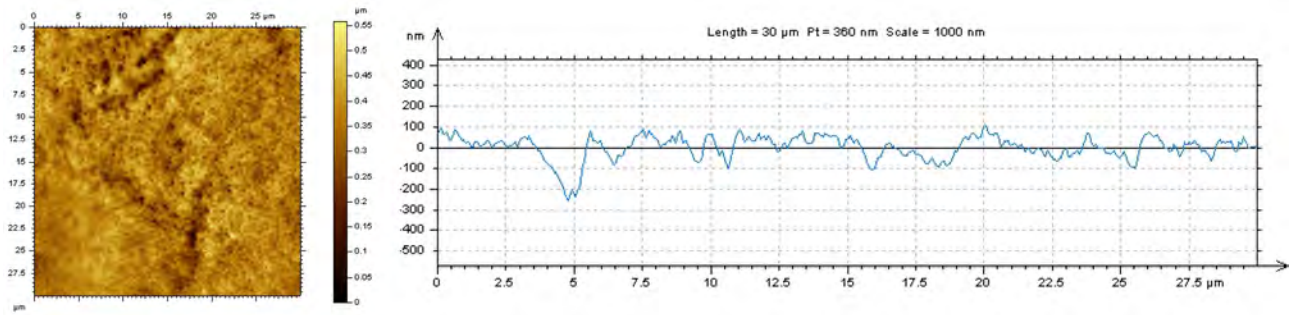

Fig. 11. 2D and 1D profiles of the cyan ink surface printed on a transparency film, measured by AFM.

This roughness profile was then used to predict the reflection of electromagnetic waves of frequencies covering the visible spectrum on the inked film. Two prediction models were used: the finite element method (FEM)[23], and the rigorous coupled-wave analysis method (RCWA) extended to non-binary and non-periodical roughness pattern[24-25]. The 45°:45° geometry was considered. Since this angle is very close to the Brewster angle, the TM polarization component is almost not reflected and only the reflection of the TE polarization component was predicted. The refractive indices of the ink and of the film are the ones plotted in Fig. 7. With both models, two predictions were performed by considering either a flat ink-air interface (in this case, the model is equivalent to a thin film model with flat interfaces), of a rough ink-air interface. The four predicted spectra are plotted in Fig. 12. For a flat surface, the FEM and RCWA models predict almost identical spectra. For a rough surface, with the same roughness profile, the two models predict very similar spectra differing only by a constant scaling factor.

In order to compare the spectral reflectance distribution predicted by these models and the measured one, we measured the spectral reflectance factor of the inked film by illuminating it at 45° with collimated light from a halogen source and placing an Ocean Optics USB2000 spectrophotometer in the specular direction. Since the perfectness of the collimation of light is difficult to assess, the γ factor defined in Section 2.2, thereby the scale of the measured spectrum, is undetermined. We therefore plotted it twice with two different scales, fitted in order to match the prediction obtained with a flat surface on the one hand (grey line), and the prediction obtained with a rough surface on the other hand (black line).

Between 500 and 700 nm, for both flat and rough surfaces, the matching between predicted and measured spectra is not perfect but good enough to consider that the modelization approach is correct. The strong deviations observed beyond 700 nm remains unexplained, but they might have a rather weak impact on color since the color matching functions are low in this spectral domain. A strong deviation is also observed below 500 nm with the flat surface models, similar to the deviation that was noticed in Fig. 9 with the inked glossy paper. It is interesting to see that with the rough surface, the deviation in this spectral domain is smaller, and concentrated around 500 nm. As expected after Ament[9], the thin roughness tends to attenuate the very-specular reflectance, due to wave scattering, by a factor of the form $1-(p/\lambda)^2$ where p is a constant related to the refractive index of the ink and the roughness. The attenuation is therefore stronger for the short wavelengths that the long wavelength.

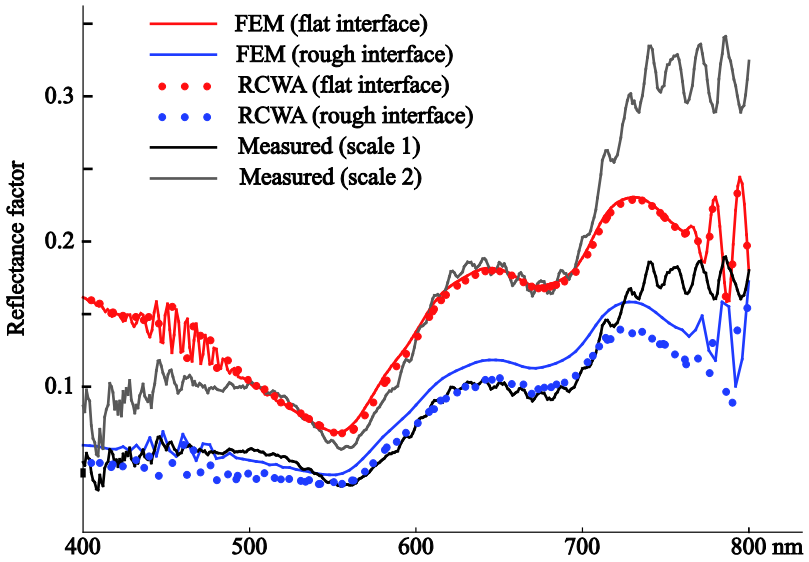

Fig. 12. Spectral reflectance factor of a transparency film coated with cyan ink, predicted according to the Finite Element Method (solid lines) and the Rigorous Coupled-Wave Analysis method (dots), for a 45°:45° geometry, by considering either a flat (red lines or dots) or a rough (blue lines or dots) air-ink interface. The measured reflectance (black and grey lines) is duplicated and rescaled in order to obtain the best matching with the predicted spectra for the two types of interfaces.

6. CONCLUSIONS

This work is a first exploration of bronzing, or gloss differential. Although not complete, it draws the main characteristic of the phenomenon: its spectral power distribution, and its magnitude depending on the illumination geometry. Our experiments tend to show that it relies on the effect of the spectral variation of the complex refractive index of the ink on the reflectance of the ink-air interface. By replacing in the Clapper-Yule model the specular reflectance component usually predicted by assuming a real, wavelength-independent refractive index of ink with the one predicted with the spectral complex refractive index, we improve its capacity of predicting the specular reflectance of an inked glossy paper in the diffuse:8° geometry. For collimated light, our results are less satisfying because the measurements are more imprecise and the bronzing effect is emphasized. The electromagnetic models that we tested despite the heavy computational effort they need, are interesting because they can predict the attenuation of the short wavelengths in the specular direction. Other models can be also developed on the bases of multilayer and thin film theories, hoping that the prediction accuracy is improved with a still acceptable model complexity. With a deeper comprehension of the phenomenon, we might expect that spectral reflectance prediction model will be improved, especially on the specific question of overprinting which is still a challenging subject for scientist in the color reproduction domain.

7. ACKNOWLEDGMENTS

This work was supported by the French National Research Agency (ANR) within the program " Investissements d'Avenir" (ANR-11-IDEX-0007), in the framework of the LABEX MANUTECH-SISE (ANR-10-LABX-0075) of Université de Lyon.

REFERENCES

[1] "Bronzing on Inkjet Paper", Image Science, 22 August 2011, http://www.imagescience.com.au/kb/questions/57/Bronzing+on+Inkjet+Paper.
[2] Wildeman, S., "Specular colors," φ^2, 31 December 2011, http://www.phikwadraat.nl/specular_colors.
[3] Born, M., Wolf, E., [Principle of Optics, 7th Edition], Pergamon, Oxford (1999).
[4] Clapper, F. R., Yule, J. A. C.; "The Effect of Multiple Internal Reflections on the Densities of Halftone Prints on Paper," *Journal of the Optical Society of America* 43, 600–603 (1953).
[5] CIE, "Colorimetry," CIE Technical Report 15, 3rd ed. (CIE, 2004)
[6] Nicomedus, F.E., Richmond, J.C., Hsia, J.J., "Geometrical considerations and nomenclature for reflectance," NBS Monograph 160, NBS, 52 (1977).
[7] NPIRI Color Measurement Task Force, "A method for the identification and assessment of the presence of bronzing in printing ink films," *American Ink Maker* 79(10), 99-104 (2001).
[8] Williams, F.C., Clapper, F.R., "Multiple Internal Reflections in Photographic Color Prints," J Opt. Soc. Am 29, 595–599 (1953).
[9] Ament, W.S., "Toward a theory of reflection by a rough surface," Proc. IRE, 41, 142-146 (1953).
[10] Ogilvy, J. A., [Theory of wave scattering from random rough surfaces], Institute of Physics Publishing, Bristol and Philadelphia (1991).
[11] Hébert, M., Hersch, R. D., Emmel, P., " Fundamentals of optics and radiometry for color reproduction" in [Handbook of Digital Imaging], Ed. Kriss, M., Wiley, New-York, 2015.
[12] Azzam, R. M. A., Bashara, N. M., [Ellipsometry and polarized light, 3rd edition], North Holland (1988).
[13] Hébert, M., Emmel, P., "Two-flux and multi-flux matrix models for colored surfaces," in [Handbook of Digital Imaging], Ed. Kriss, M., Wiley, New-York, 2015.
[14] Wyszecki, G., Stiles, W.S., [Color science: Concepts and methods, quantitative data and formulae, 2nd edition], Wiley, New York (1982).
[15] Hébert, M., Hersch, R. D., "Classical Print Reflection Models: A Radiometric Approach," J. Im. Sci. Technol. 48, 363-374 (2004).
[16] Judd, D. B., "Fresnel reflection of diffusely incident light," J. Research of the National Bureau of Standards 29, 329-332 (1942).
[17] Simonot, L., Hébert, M., Hersch, R. D., "Extension of the Williams-Clapper model to stacked nondiffusing colored layers with different refractive indices," J. Opt. Soc. Am. A 23, 1432-1441 (2006).

[18] Hébert, M., Hersch, R.D., "Deducing ink-transmittance spectra from reflectance and transmittance measurements of prints," Proc. SPIE 6493, 649314-1-13 (2007).
[19] Centurioni, E., " Generalized matrix method for c alculation o f in ternal l ight e nergy flux i n mixed coherent a nd incoherent mul tilayers," Appl. Opt. 44, 7532-7539 (2005).
[20] Cook, R.L., Torrance, K.E., "A Reflectance Model for Computer Graphics," ACM Transactions On Graphics 1, 7–24 (1982).
[21] Smith, B.G., "Geometrical shadowing of a random rough surface," *IEEE Transaction on Antennas and Propagation*, **15**, 668–671 (1967).
[22] Hébert, M., Hersch, R. D., "Extending the Clapper-Yule model to rough printing supports," J. Opt. Soc. Am. A 22, 1952-1967 (2005).
[23] Hugonin, J. P., Besbes, M., Lalanne, P., "Hybridization of electromagnetic numerical methods through the G-matrix algorithm," Opt. Lett. 33, 1590-1592 (2008).
[24] Hugonin, J.-P., Lalanne, P., "Perfectly matched layers as nonlinear coordinate transforms: a generalized formalization," J. Opt. Soc. Am. A **22**, 1844-1849 (2005).
[25] Moharam, M . G ., G aylord, T . K ., G rann, E . B ., P ommet, D . A ., " Formulation f or s table a nd efficient implementation o f th e r igorous c oupled-wave a nalysis of binary gr atings," J . O pt. S oc. A m. A 12, 1 068-1076 (1995).